

# Dependence of Crystallinity and Crystallite Size of Hydroxyapatite from Chicken Eggshell on Calcination Time: A Comparative Study on Scherrer Approach

Ya' Muhammad Arsyad¹\*, Mega Nurhanisa ¹٬², Elsa Narulita², Ayunda Dwi Handayani², Frinelda Rehulina Barus², Tri Rahma Febrianti Maharani², Hilyana Agis Risla², Latifah Tri Amanda², Delia Amanda², Zahraini Tasya Siregar²

<sup>1</sup> Advanced and Computational Physics Laboratory, Universitas Tanjungpura, Indonesia

<sup>2</sup> Department of Physics, Universitas Tanjungpura, Indonesia

#### ARTICLE INFORMATION

Article Histories: Submitted: 17 April 2025 Revision: 22 July 2025 Accepted: 7 August 2025 Published: 24 October 2025

Corresponding author: <a href="mailto:yamarsyad@qmail.com">yamarsyad@qmail.com</a>

#### **ABSTRACT**

The increasing demand for bone graft materials has driven the development of synthetic alternatives that closely mimic the mineral structure of natural bone and dental tissues. Hydroxyapatite (HAp) is a calcium phosphate material whose crystal structure closely resembles that of bone and dental tissue, making it highly suitable for various biomedical applications. In this study, calcium oxide (CaO) was obtained from calcined chicken eggshells, with calcination durations of 2, 3, and 4 hours, followed by the synthesis of HAp using the hydrothermal method at 160°C for 24 hours. X-ray diffraction (XRD) analysis was performed to evaluate the effects of calcination time on crystallinity and crystallite size. The results showed that increasing the calcination time led to higher crystallinity, ranging from 46% to 54%. Crystallite size was estimated using three Scherrer-based methods. The straight-line Scherrer method produced values ranging from 1733.17 to 4621.8 nm, the average Scherrer method from 11.33 to 11.74 nm, and the modified Scherrer method from 8.49 to 9.11 nm. All three methods consistently indicated a decrease in crystallite size with longer calcination durations. These findings demonstrate that prolonged calcination enhances crystallinity and reduce crystallite size, underscoring the critical role of calcination time in shaping structural characteristics of HAp.

Keywords: Hydroxyapatite, Chicken Eggshell, Scherrer Approaches, XRD.

## 1. INTRODUCTION

Hydroxyapatite (HAp) with the molecular formula  $Ca_{10}(PO_4)_6(OH)_2$  is a calcium phosphate biomaterial whose crystal structure closely resembles that of human bone tissue, allowing it to integrate effectively with bone [1]. Its biocompatibility, bioactivity, strong affinity for body tissues make HAp widely used as a biomaterial for bone implants [2], [3]. HAp can be synthesized from biogenic sources derived from biomass waste containing calcium[4]. The use of biogenic materials as raw materials for HAp production offers advantages in reducing production costs and minimizing environmental impacts compared to synthetic calcium sources. One of the potential household waste is chicken eggshells (CES). CES contains calcium in the form of calcium carbonate (CaCO<sub>3</sub>) as the main composition of 94% [5]. Therefore, CES represent a highly potential biogenic source for synthesizing HAp.

The production of HAp from biogenic sources generally requires a calcination step at high temperatures to convert CaCO<sub>3</sub> into calcium oxide (CaO). One of the key parameters that affect the physical and chemical properties of HAp is the duration of calcination. Previous studies have shown that calcination time influences the phase composition and the calcium-to-phosphate (Ca/P) ratio of the final product [6], [7]. In addition, varying the calcination time has been reported to improve HAp yield up to 83% at 180 minutes [8]. A calcination time in the range of 4-6 hours also contributed to increasing the purity up to 65.36%, crystallinity up to 88.20%, and crystal size up to 47.73 nm [9]. Therefore, this study investigates calcination time as a variable that affects the characteristics of the synthesized HAp. In addition to calcination time, the synthesis method used for producing HAp also affects the final results of HAp formation. Several methods have been utilized for the synthesis of Hap, including precipitation, sol-gel, hydrothermal, and multiple emulsion methods [10]. The hydrothermal method is widely used to produce pure HAp particles from biogenic sources under high-pressure and high-temperature conditions to achieve thermodynamic equilibrium [11], which facilitates the formation of well-crystallized HAp and allows better control over crystallite size.

X-ray Diffraction (XRD) is a widely used characterization technique to verify the phase composition of HAp, as well as to estimate its crystallinity and crystallite size [12]. Among the various approaches used to calculate crystallite size from XRD data,

the Scherrer equation remains one of the most commonly applied, as it relates peak broadening to the size of coherently scattering domains. Several Scherrer-based methods currently employed include the straight-line, average, and modified Scherrer approaches [13]. Nevertheless, most studies tend to rely solely on the average Scherrer method, which may limit broader insight into how calcination time influences crystallite refinement. Comparative use of these three approaches allows for a more comprehensive evaluation of time-dependent crystallite evolution. In particular, the modified Scherrer approach introduced by Monsi in 2012 offers a potentially more refined estimation [14], especially when microstructural changes occur progressively with extended thermal treatment.

Based on this background, this study aims to synthesize HAp from CES by varying the calcination time and evaluating its influence on the resulting crystallinity and crystallite size through XRD analysis. This study also compares crystallite size estimations using three Scherrer-based approaches. The findings are expected to support the development of more accurate crystallite size estimation methods derived from the Scherrer equation, particularly for potential biomedical applications.

#### 2. RESEARCH METODOLOGY

#### 2.1 Materials

The materials utilized in this study comprised chicken eggshells (CES) obtained from household waste, technical grade sodium hydroxide (NaOH), ammonium dihydrogen phosphate  $[(NH_4)H_2PO_4]$  (99% purity, Merck), ammonium hydroxide (NH<sub>4</sub>OH) solution (25% concentration, Merck), and distilled water as the solvent.

## 2.2 Synthesis Route of Hap from CES

The synthesis route of HAp from CES, including CaO preparation and HAp formation, is illustrated in Figure 1. The collected CES were initially cleaned to remove any remaining inner membranes. Subsequently, the CES were thoroughly washed with water to eliminate adhering impurities. The cleaned shells were sun-dried to remove residual moisture. After drying, the CES were immersed in a 5% (w/v) NaOH solution for 1 hour to dissolve any remaining organic contaminants. Following this treatment, the CES were rinsed again with water to ensure the complete removal of residual alkali, then dried to a constant weight. The dried CES were ground using a grinder to obtain a fine powder, which was then sieved through a 200-mesh sieve to achieve a uniform particle size distribution. Calcination was performed in a furnace at 1000°C with varying holding times of 2, 3, and 4 hours to convert the calcium carbonate (CaCO<sub>3</sub>) present in the eggshells into CaO, as represented by Equation (1).

$$CaCO3(s) \rightarrow CaO(s) + CO2(g)$$
(1)

A total of 5 grams of CaO powder was added to 15 mL of 2 Molar ( $NH_4$ )  $H_2PO_4$  solution. The suspension was stirred with a magnetic stirrer until it was homogeneous. The pH was adjusted with 3M of  $NH_4OH$  until reaching 11–12, as measured by a pH meter. The suspension was then transferred into an autoclave for hydrothermal treatment at 160 °C for 24 h to promote HAp formation. After natural cooling to ambient temperature, the suspension was recovered by filtration and washed with deionized water until the filtrate reached a neutral pH (7–8) to remove residual ions and impurities. Finally, the precipitate was dried in an oven at 110 °C until the filtrate reached a constant mass.

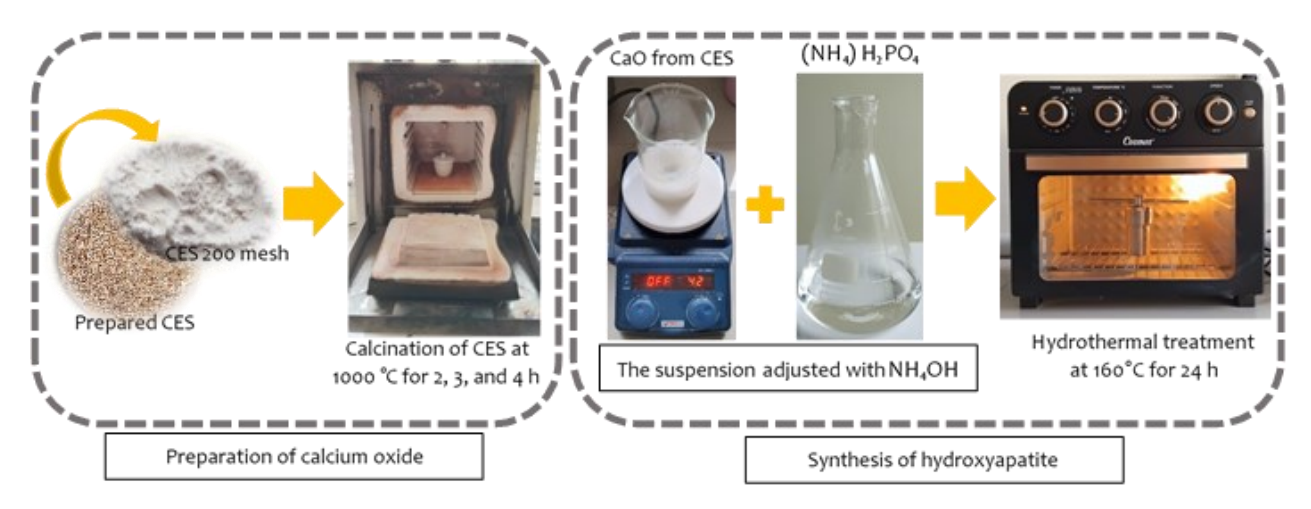


Figure 1. Experimental procedure for synthesis of HAp

#### 2.3 XRD Characterization and Data Analysis

Characterization of the synthesized HAp samples was performed using XRD. XRD measurements were carried out on a diffractometer. The resulting data were analysed using Origin software and Microsoft Excel to determine both the degree of crystallinity and the crystallite size. The experimental procedure is illustrated in Figure 2.

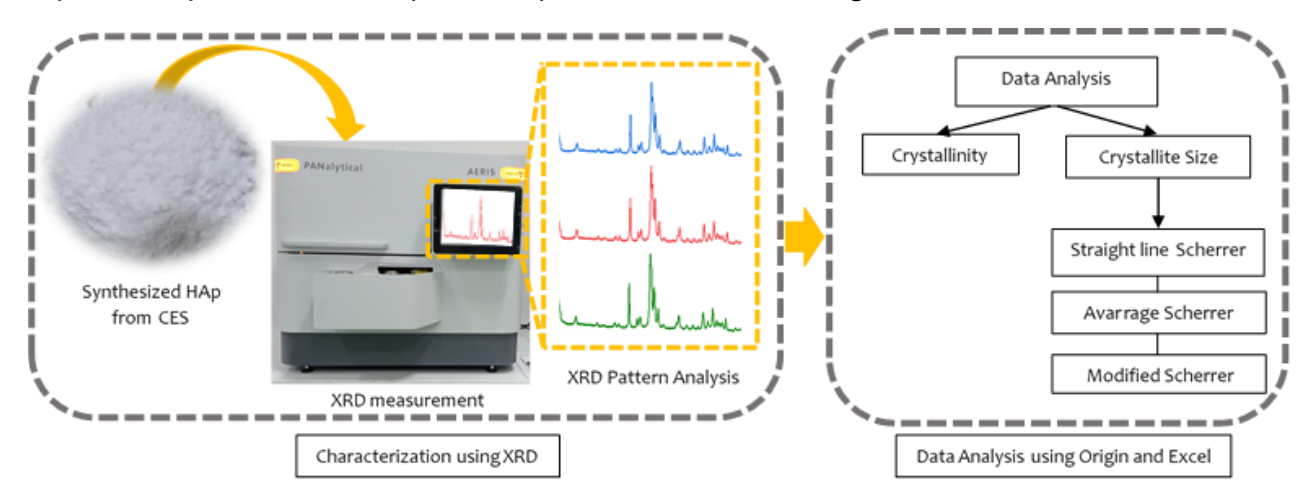


Figure 2. Experimental procedure for characterization and data analysis of synthesized HAp

Mathematically, the degree of crystallinity was calculated using Equation (2).

$$C = \frac{A_c}{A_c + A_a} \times 100\% \tag{2}$$

C represents the degree of crystallinity (%), where  $A_c$  denotes the total area of the crystalline peak, and  $A_a$  refers to the total area of the amorphous peak.

#### 2.4 Scherrer Approaches Method

In this study, the crystallite size was assessed by comparing three approaches of the Scherrer method as mentioned in Figure 2. The first method applied the straight line Scherrer approach by plotting  $1/\beta$  against  $\cos\theta$ , and crystal size was measured using the slope of linear fit. The second approach uses Equation (3) to calculate the crystal size of a sample and average the value across samples.

$$D = \frac{K\lambda}{\beta\cos\theta} \tag{3}$$

Third, the Monshi-Scherrer equation is derived from the natural logarithmic transformation of the Scherrer equation, resulting in a linear relationship between  $\ln \beta$  and  $\ln (1/\cos \theta)$ . Mathematically, the Monshi-Scherrer equation can be expressed as shown in Equation (4)

$$\ln \beta = \ln \frac{1}{\cos \theta} + \ln \frac{K\lambda}{D} \tag{4}$$

By utilizing the intercept in the linear correlation, the crystallite size can be determined using Equation (5)

$$D = \frac{K\lambda}{\rho^{in}} \tag{5}$$

Where D is the crystallite size (nm), K is the Scherrer constant (0.9),  $\lambda$  is the wavelength of the X-ray source (1.5406 Å),  $\beta$  is the full width at half maximum (FWHM, in radians), and  $\theta$  is the diffraction peak position (degree),  $e^{in}$  represents the exponent of the intercept derived from the Monshi-Scherrer plot.

## 3. RESULTS AND DISCUSSION

# 3.1 Mass Loss Analysis of CaO

The mass loss percentage of CaO during calcination is presented in Figure 3. The measurement results indicate a notable increase in mass loss as the calcination time progresses. At a calcination duration of 2 hours, the mass loss remains relatively low compared to other variations. This is attributed to the initial dehydration process and the evaporation of water and residual volatile compounds from the precursor material, suggesting that the decomposition of CaCO<sub>3</sub> has not yet been completed. An increase in mass loss is observed at a calcination time of 3 hours, with a rise of approximately 44% compared to the previous duration. This sharp increase indicates that the most intensive decomposition of CaCO<sub>3</sub> into CaO occurs at this stage, characterized by the substantial release of CO<sub>2</sub> gas, leaving behind Ca and O elements in the form of CaO, which can subsequently act as precursor compounds for the synthesis of HAp [15]. At a calcination time of 4 hours, the mass loss increases by only 3% compared to the 3-hour mark. This phenomenon suggests that the majority of the decomposition process is completed within the first 3 hours, while the subsequent phase primarily involves the decomposition of residual carbonates or other minor impurities that may influence the purity of HAp. This indicates that the CES reaches a relatively stable thermal state by the fourth hour of calcination. Nonetheless, mass loss is expected to continue with prolonged calcination. For instance, extending the calcination of CES to 5 hours results in mass loss up to 56.40% [16].

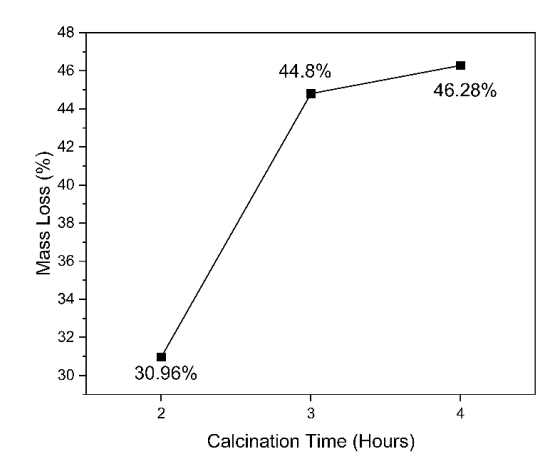


Figure 3. Mass loss analysis of CES after calcination with various time

#### 3.2 XRD Diffractogram and Crystallinity of HAp

The XRD diffractogram presented in Figure 4 confirms the formation of the HAp phase from CES synthesized via the hydrothermal method. The three variations in calcination time, labeled C2, C3, and C4 corresponding to 2, 3, and 4 hours respectively, exhibit a dominant diffraction peak at  $2\theta = 31.95^{\circ}$ . This value is in close agreement with the standard HAp peak reported in previous studies, which appears at  $2\theta = 31.78^{\circ}$  [17]. Additional diffraction peaks supporting the presence of HAp in all three samples are observed at  $2\theta$  values of  $26.04^{\circ}$ ,  $32.33^{\circ}$ ,  $34.24^{\circ}$ , and  $49.64^{\circ}$ , which are also consistent with those reported in prior research on HAp synthesized from *Geloina coaxans* [8].

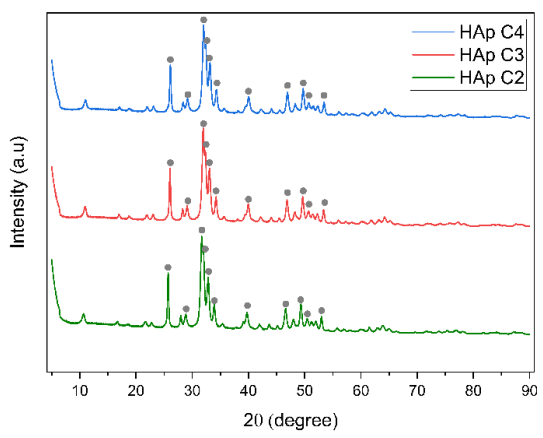


Figure 4. XRD pattern of HAp with various calcination time

Based on the XRD diffractogram shown above, the percentage of crystallinity was calculated using Equation (2). As presented in Table 1, HAp samples subjected to longer calcination times exhibited higher crystallinity. This can be attributed to the reduction in CaO particle size induced by prolonged calcination [18], which promotes crystallite growth supported by improved crystallization at temperatures around 160 °C during synthesis [19], resulting in higher crystallinity. Additionally, extended calcination duration enhances the purity of HAp, as more impurities are removed during the process. The reduction of residual phases or volatile components at this temperature contributes to the formation of a more well-defined and ordered crystal structure, thereby increasing the overall crystallinity of the material [20]. In addition to calcination time, a hydrothermal synthesis temperature of 160 °C, as reported in previous studies, has been shown to produce HAp with minimal impurities and high crystallinity [21]. In the present study, the crystallinity percentage ranged from 46% to 54%, which is lower than the value reported for HAp synthesized from CES in previous research, which was 56.46% at a hydrothermal temperature of 230 °C [22].

Table 1. Crystallinity of HAp from CES

No	Time variation	Crystallinity (%)
1	HAp C2	46.79
2	HAp C3	52.44
3	HAp C4	54.45

## 3.3 Crystallite sizes of HAp

# 1. Straight Line Scherrer Method

The determination of crystallite size in this study was carried out by comparing three approaches based on the Scherrer method. The first approach utilizes a straight-line model derived from the Scherrer equation. In this method, crystallite size is determined through linear graph analysis by plotting  $1/\beta$  against  $\cos\theta$  to obtain the slope value as shown in Figure 5. A straight line fitting is applied to establish a mathematical relationship that enables the quantitative calculation of crystallite size using the Scherrer equation, as presented in Equation (3). The slope of the resulting line is equal to the Scherrer constant multiplied by the X-ray wavelength, divided by the crystallite size.

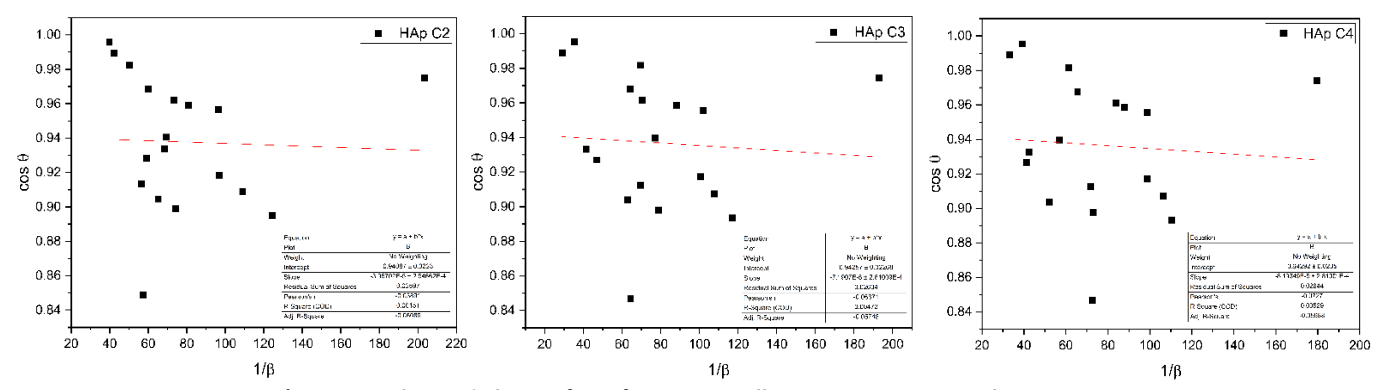


Figure 5. Scherrer's linear fits of HAp crystallite size at various calcination times

The slope values obtained from samples C2, C3, and C4 were 0.00003, 0.00007, and 0.00008, respectively. Based on these slopes, the calculated crystallite sizes were 4621.8 nm, 1980.77 nm, and 1733.17 nm. However, these values deviate from the typical crystallite size range commonly observed in XRD analysis, suggesting that they may not accurately represent the true crystallite size. This indicates that the straight-line Scherrer approach lacks precision in determining crystallite size, as also reported in previous studies [13], [23].

#### 2. Average Scherrer Method

The second approach employs the conventional Scherrer equation, in which the crystallite size is calculated for each of the main diffraction peaks and then averaged to obtain an overall value. The detailed calculation results are presented in Table 2. Based on this method, the crystallite sizes were found to be in the range of 4–28 nm, with the average crystallite size across the three sample variations being approximately ~11 nm. These results are more consistent, indicating that this approach provides a reliable estimation of crystallite size. Nevertheless, this crystallite sizes obtained in this study is relatively smaller than those reported for other biogenic sources using the average Scherrer method, such as sand lobster at 70.93 nm [23], cockle shells around 54.19 nm[24], green mussel shell approximately 34.58 nm [20], and camel bone at 30.54 nm [25].

Table 2. Crystallite size of HAp using the average model of Scherrer equation

No -	Crystallite Size (nm)			
NO	C2	C3	C4	
1	5.53	4.93	5.45	
2	5.93	4.05	4.65	
3	7.06	9.80	8.65	
4	28.95	27.46	25.57	
5	8.59	9.21	9.38	
6	10.56	10.16	12.11	
7	11.69	12.76	12.71	
8	13.94	14.81	14.34	
9	10.21	11.35	8.38	
10	10.17	6.14	6.30	
11	8.84	7.01	6.14	
12	14.61	15.20	14.92	
13	8.55	10.55	10.92	
14	16.63	16.48	16.26	
15	9.97	9.62	7.99	
16	11.45	12.17	11.25	
17	19.28	18.18	17.11	
18	9.34	10.54	11.90	
Average	11.74	11.69	11.33	

## 3. Modified Scherrer Method

The third approach utilizes the modified Scherrer method, commonly known as the Monshi–Scherrer method. This method applies linear fitting to logarithmic data (Figure 6) to obtain the intercept value, which is then used to estimate the crystallite size. The use of multiple diffraction peaks in the Monshi–Scherrer method helps to minimize the effects of small variations caused by FWHM measurement inaccuracies or signal interference, thereby providing a more stable and reliable estimation of crystallite size. In this study, the intercept values obtained exhibited a systematic change with increasing calcination time, yielding –4.18517, –4.11718, and –4.11469 for samples C2, C3, and C4, respectively. These values reflect a consistent trend associated with prolonged calcination. Based on Equation (5), the crystallite sizes calculated using this method were 9.11 nm, 8.51 nm, and 8.49 nm. The obtained values are lower than those typically reported using the average Scherrer method, which has been extensively applied for estimating crystallite size. This observation is further supported by previous studies, which indicate that the modified Scherrer method generally yields smaller crystallite sizes compared to the average-based approach [25].

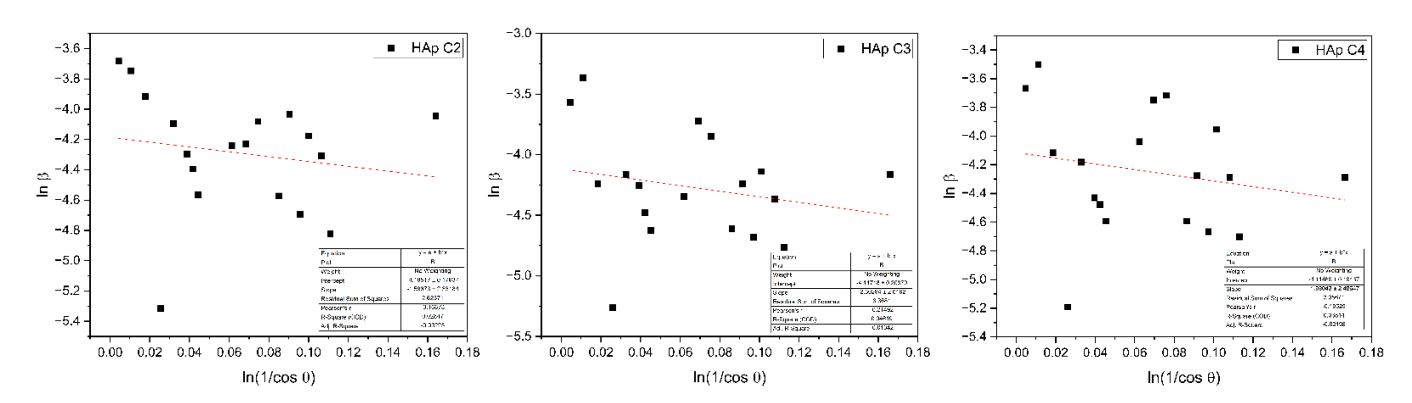


Figure 6. Monshi–Scherrer linear fits of HAp crystallite size at various calcination times

Despite the differences in the crystallite size values obtained from the three approaches, a consistent trend is observed: crystallite size tends to decrease with increasing calcination time. Previous studies have reported that prolonged calcination promotes lattice rearrangement and particle coalescence, which reduce lattice strain and result in smaller apparent crystallite sizes [20]. This process may allow atomic redistribution at grain boundaries, not only relieving internal stress but also fragmenting larger crystallites into smaller domains. In addition, nonuniform and limited grain boundary movement, possibly due to the presence of secondary phases or crystal defects, may hinder grain growth and instead promote recrystallization into finer crystalline domains. The observed reduction in crystallite size is further supported by the Scherrer method, which is highly sensitive to lattice strain and microstructural defects. Nevertheless, the conventional Scherrer method presents a limitation due to its inability to capture

the systematic relationships among diffraction parameters. In comparison, the Monshi–Scherrer method utilizes linear regression across multiple diffraction peaks, enhancing statistical reliability and yielding a more representative estimation of crystallite size. By employing the least squares fitting technique, the modified Scherrer approach effectively minimizes errors arising from instrumental broadening and data variability, thus providing a more accurate determination of crystallite size [14].

### 4. CONCLUSION

This study has demonstrated that HAp synthesized from CES-derived calcium exhibits a time-dependent structural evolution, specifically concerning calcination time. XRD analysis showed that mass loss and crystallinity increased with prolonged calcination, with the highest crystallinity obtained in this study being approximately 54.45% at a calcination duration of 4 hours. Concurrently, the crystallite size, as determined via three Scherrer-based approaches, decreased consistently with longer calcination times. These results highlight the critical role of calcination time in determining the crystallinity and crystallite size of CES-derived HAp. Time-controlled calcination thus emerges as a key parameter for optimizing HAp properties tailored to specific applications, such as bone graft substitutes, implant coatings, and environmental remediation. Future investigations are encouraged to utilize other characterization techniques to evaluate how calcination time affects its physicochemical and mechanical properties of HAp for biomaterial applications.

## 5. REFERENSI

- [1] V. S. Kattimani, S. Kondaka, and K. P. Lingamaneni, "Hydroxyapatite—Past, Present, and Future in Bone Regeneration," Bone Tissue Regen. Insights, vol. 7, no. November, p. BTRI.S36138, 2016.
- [2] H. Shi, Z. Zhou, W. Li, Y. Fan, Z. Li, and J. Wei, "Hydroxyapatite based materials for bone tissue engineering: A brief and comprehensive introduction," *Crystals*, vol. 11, no. 2, pp. 1–18, 2021.
- [3] I. Ielo, G. Calabrese, G. De Luca, and S. Conoci, "Recent Advances in Hydroxyapatite-Based Biocomposites for Bone Tissue Regeneration in Orthopedics," *Int. J. Mol. Sci.*, vol. 23, no. 17, 2022.
- [4] Y. Yusuf, D. U. Khasanah, F. Y. Syafaat, I. Pawarangan, M. Sari, and V. J. Mawuntu, "Hidroksiapatit berbahan dasar biogenik," *Gadjah Mada Univ. Press*, no. June 2023, pp. 117–130, 2019.
- [5] A. R. Noviyanti *et al.*, "A novel hydrothermal synthesis of nanohydroxyapatite from eggshell-calcium-oxide precursors," *Heliyon*, vol. 6, no. 4, p. e03655, 2020.
- [6] S.-C. Wu, H.-C. Hsu, S.-K. Hsu, C.-P. Tseng, and W.-F. Ho, "Effects of calcination on synthesis of hydroxyapatite derived from oyster shell powders," *J. Aust. Ceram. Soc.*, vol. 55, no. 4, pp. 1051–1058, 2019.
- [7] A. R. Nurhidayat, A. P. Bayuseno, R. Ismail, and R. B. Taqriban, "Review of the temperature and holding time effects on hydroxyapatite fabrication from the natural sources," *J. Biomed. Sci. Bioeng.*, vol. 1, no. 1, pp. 27–31, 2021.
- [8] P. H. Yanti and Y. Gandi, "Pengaruh Waktu Kalsinasi Terhadap Sifat Fisika-Kimia Hidroksiapatit Dari Cangkang Geloina Coaxans," Chem. Prog., vol. 13, no. 2, pp. 102–106, 2020.
- [9] E. D. Prasetyawan, "Pengaruh Waktu Kalsinasi Pada Sintesis Hidroksiapatit Berbasis Cangkang Telur Ayam Untuk Aplikasi Biomaterial," *Jtm*, vol. 2, pp. 17–22, 2023.
- [10] A. K. Nayak, "Hydroxyapatite Synthesis Methodologies: An Overview," Int. J. ChemTech Res., vol. 2, no. 2, pp. 903–907, 2010.
- [11] B. S. Nugroho, D. Wahyuni, A. Asri, and A. Lirawanto, "Effects Of Calcination Temperature on Ca/P Ratio of Calcium Phosphate from Freshwater Snails (Sulcospira Testudinaria) Shells," *J. Phys. Conf. Ser.*, vol. 2945, no. 1, pp. 1–6, 2025.
- [12] G. M. Poralan, J. E. Gambe, E. M. Alcantara, and R. M. Vequizo, "X-ray diffraction and infrared spectroscopy analyses on the crystallinity of engineered biological hydroxyapatite for medical application," *IOP Conf. Ser. Mater. Sci. Eng.*, vol. 79, no. 1, 2015.
- [13] M. Rabiei, A. Palevicius, A. Monshi, S. Nasiri, A. Vilkauskas, and G. Janusas, "Comparing methods for calculating nano crystal size of natural hydroxyapatite using X-ray diffraction," *Nanomaterials*, vol. 10, no. 9, pp. 1–21, 2020.
- [14] A. Monshi, M. R. Foroughi, and M. R. Monshi, "Modified Scherrer Equation to Estimate More Accurately Nano-Crystallite Size Using XRD," World J. Nano Sci. Eng., vol. 02, no. 03, pp. 154–160, 2012.
- [15] N. A. S. Mohd Pu'ad, J. Alipal, H. Z. Abdullah, M. I. Idris, and T. C. Lee, "Synthesis of eggshell derived hydroxyapatite via chemical precipitation and calcination method," *Mater. Today Proc.*, vol. 42, no. January 2021, pp. 172–177, 2019.
- [16] F. S. Irwansyah, A. F. R. Nurizal, E. P. Hadisantoso, and S. B. M. Zain, "Characterization and Application of Hydroxyapatite From Chicken Egg Shell with Green Template as a Potential Drug Delivery System," *J. Kim. Val.*, vol. 10, no. 2, pp. 260–268, 2024.

- [17] N. H. Thang and D. T. Phong, "Characterizations of hydroxyapatite synthesized from calcium hydroxide and phosphoric acid as adsorbents of lead in wastewater," *Mater. Sci. Forum*, vol. 991 MSF, pp. 159–165, 2020.
- [18] A. Putkham, S. Ladhan, and A. I. Putkham, "Changing of particle size and pore structures of calcium oxide during calcinations of industrial eggshell waste," *Mater. Sci. Forum*, vol. 998 MSF, pp. 90–95, 2020.
- [19] N. Méndez-Lozano, M. Apátiga-Castro, K. M. Soto, A. Manzano-Ramírez, M. Zamora-Antuñano, and C. Gonzalez-Gutierrez, "Effect of temperature on crystallite size of hydroxyapatite powders obtained by wet precipitation process," *J. Saudi Chem. Soc.*, vol. 26, no. 4, 2022.
- [20] C. Rachmantio and M. A. Irfai, "Pengaruh Suhu Dan Waktu Kalsinasi Terhadap Kemurnian Hidroksiapatit Berbasis Cangkang Kerang Hijau Untuk Aplikasi Pada Bone Tissue Engineering," *Jtm*, vol. 11, no. 1, pp. 1–6, 2023.
- D. F. Fitriyana *et al.*, "The Effect of Temperature on the Hydrothermal Synthesis of Carbonated Apatite From Calcium Carbonate Obtained From Green Mussels Shells," ARPN J. Eng. Appl. Sci., vol. 18, no. 11, pp. 1215–1224, 2023.
- [22] A. Yusuf, N. M. Muhammad, A. R. Noviyanti, and Risdiana, "The effect of temperature synthesis on the purity and crystallinity of hydroxyapatite," *Key Eng. Mater.*, vol. 860 KEM, pp. 228–233, 2020.
- [23] A. H. Diputra, I. K. Hariscandra Dinatha, and Y. Yusuf, "A comparative X-ray diffraction analysis of Sr2+substituted hydroxyapatite from sand lobster shell waste using various methods," *Heliyon*, vol. 11, no. 2, p. e41781, 2025.
- Y. Rizkayanti and Y. Yusuf, "Effect of temperature on syntesis of hydroxyapatite from cockle shells (Anadara Granosa)," *Int. J. Nanoelectron. Mater.*, vol. 11, no. April, pp. 43–50, 2018.
- [25] S. Rahavi, A. Monshi, R. Emadi, A. Doostmohammadi, and H. Akbarian, "Determination of crystallite size in synthetic and natural hydroxyapatite: A comparison between XRD and TEM results," *Adv. Mater. Res.*, vol. 620, pp. 28–34, 2013.